Relaxation dynamics in the presence of pulse multiplicative noise sources with different correlation properties

A. V. Kargovsky* and O. A. Chichigina
Faculty of Physics and International Laser Center, Lomonosov Moscow State University, Leninskie Gory, 119992 Moscow, Russia

E. I. Anashkina
Faculty of Physics, Lomonosov Moscow State University, Leninskie Gory, 119992 Moscow, Russia
and Dipartimento di Fisica e Chimica, Group of Interdisciplinary Theoretical Physics, Università di Palermo, Viale delle Scienze, Edificio 18, 90128 Palermo, Italy

D. Valenti and B. Spagnolo
Dipartimento di Fisica e Chimica, Group of Interdisciplinary Theoretical Physics, Università di Palermo and CNISM, Unità di Palermo, Viale delle Scienze, Edificio 18, 90128 Palermo, Italy
and Istituto Nazionale di Fisica Nucleare, Sezione di Catania, Italy
(Received 16 June 2015; published 20 October 2015)

The relaxation dynamics of a system described by a Langevin equation with pulse multiplicative noise sources with different correlation properties is considered. The solution of the corresponding Fokker-Planck equation is derived for Gaussian white noise. Moreover, two pulse processes with regulated periodicity are considered as a noise source: the dead-time-distorted Poisson process and the process with fixed time intervals, which is characterized by an infinite correlation time. We find that the steady state of the system is dependent on the correlation properties of the pulse noise. An increase of the noise correlation causes the decrease of the mean value of the solution at the steady state. The analytical results are in good agreement with the numerical ones.

DOI: 10.1103/PhysRevE.92.042140 PACS number(s): 02.50.Ey, 05.40.−a, 05.10.Gg

I. INTRODUCTION

In recent decades there has been a growing interest in the theoretical study of relaxation dynamics for systems subject to multiplicative noise [1–4]. These systems are widespread in nature and technology, and they are widely used to describe stochastic dynamics not only in physics, but also in biology and in econophysics [5–10]. Their evolution is affected by the influence of the environment, by exchanging some physical quantity as mass or energy. The dynamical behavior of these systems is described by the Langevin equation

$$\frac{dx}{dt} = -bx + x^{\gamma}\eta(t), \tag{1}$$

where $0 \leqslant \gamma < 1, x \in \mathbb{R}^{+}$, $\eta(t)$ is a random process with non-negative mean, and b is a positive constant. This equation, which describes the relaxation of the system to the steady state, can be applied in numerous fields of science. First, this equation describes the particle motion that is affected by the linear friction and random force, that can depend on the particle velocity. For example, the case of $\gamma = 0$ corresponds to the well-known equation of reflecting Brownian motion [11].

The case of the pulse random process is of particular interest for numerous applications. In fact, Eq. (1) with $\gamma = 1/2$ describes a velocity of a particle in mathematical billiard with boundaries of scatterers, with fixed mass, moving randomly or periodically. Each particle collision with the scatterer corresponds to the pulse in the noise term. In traditional models of billiard systems scatterers have infinite mass, and the particle has constant acceleration known as Fermi acceleration [12]. The saturation of the particle velocity in a more realistic model corresponds to the fact that particle reaches such a velocity that momenta of the particle and scatterer are of the same order [13]. The loss of particle energy is characterized by the first term of Eq. (1), and the velocity approaches a steady value.

Another possible application of Eq. (1) with $\gamma = 1/2$ is the particle motion in a flow. In this case x corresponds to the kinetic energy of the probe particle moving with fixed average velocity that is much higher than thermal velocity of the particle. The first term of Eq. (1) describes the effect of friction. The flow consists of particles moving independently or with some correlations. Each pulse in the second term of Eq. (1) corresponds to the probe particle collision with a particle in flow.

Equation (1) can also describe the formation of islands composed of metal particles (atoms or clusters) on a substrate [14]. The process of island growth can be divided into three steps: deposition, when preformed clusters or atoms are deposited on a substrate, diffusion, when they diffuse chaotically, and aggregation, when the particle can join the existing island, or stick together with a neighboring particle and form a new island [15]. In this case, x represents the number of particles in an individual island. The noise denotes a non-negative random pulse process, determined by the particle flux to the boundary of island. This process is considered in the regime when a cluster can escape from an island. The probability of this escape is characterized by the first term of the equation. The technology of island production allows us to change the deposition regime [16], making the deposition process more random or more periodical. An island's growth rate depends hypothetically on its shape and is taken into account by γ.

From the point of view of population dynamics, Eq. (1) describes the time evolution of a population of predators,

*kargovsky@yumr.phys.msu.ru

whose diet is based on species with quasiperiodic change of population. The prey density can be described, from the mathematical point of view, as a pulse sequence and corresponds to the second term in equation. Pulses occur only at years of anomalous increases of the prey population density. The first term of the equation represents predator extinction due to intraspecific competition; the higher the number of individuals, the faster this extinction occurs [17].

In the field of stochastic dynamical models for financial markets, the model defined by Eq. (1) is the constant elasticity of variance process introduced by Cox and Ross and then generalized as the Cox, Ingersoll, and Ross (CIR) process to describe the evolution of interest rates [18]. The CIR process is also used in the Heston model to model stochastic volatility [8,19].

Stochastic pulse trains have been modeled by Poissonian white noise and used in thermal ratchet [20], noise-induced phase transitions [21], and population dynamics [22]. Recently, the stability of a dynamical system subject to correlated pulse multiplicative noise and quasistable processes was investigated [23–25].

In this work we study the dependence of transient dynamics and the steady state solution of the model described by Eq. (1) on the correlation properties of different noise sources. Specifically, we analyze Eq. (1) in the Stratonovich sense [26] and the influence of the noise properties on the moments of $x(t)$. We consider that the system dynamics occurs at so low temperature values that the effects of thermal fluctuations can be neglected.

The organization of the paper is as follows. In Sec. II, we consider the white noise and obtain the solution of the Fokker-Planck equation for the Gaussian noise source, and analyze the master equation for the Poisson pulse process. These results can be assumed to hold also in the presence of correlated noise by suitably changing the equation parameters [25]. In Sec. III, we show that the steady mean of x can be obtained for an arbitrary noise, whose characteristics are given through its spectral density, using reduction to the Markov process. As an example, we use two pulse processes: the dead-time-distorted Poisson (DTDP) pulse process and the pulse process with fixed time intervals (FTI). Section IV is devoted to the numerical simulation of Eq. (1) and discussion of the obtained results. A summary of our results is presented in Sec. V.

II. THE EQUATION WITH WHITE NOISE

A. Gaussian white noise

Let us rewrite the Langevin equation (1) as

$$\frac{dx}{dt} = ax^{\gamma} - bx + x^{\gamma}\zeta(t), \tag{2}$$

where $\zeta(t) = \eta(t) - \langle\eta(t)\rangle$ and $\langle\eta(t)\rangle = a \geqslant 0$.

In this subsection we consider $\zeta(t)$ as the Gaussian white noise with $\langle\zeta(t)\rangle = 0$ and $\langle\zeta(t)\zeta(t')\rangle = 2D\delta(t-t')$.

The corresponding Fokker-Planck equation is

$$\frac{\partial w(x,t)}{\partial t} = -\frac{\partial}{\partial x}[(ax^{\gamma} - bx + D\gamma x^{2\gamma-1})w(x,t)] + \frac{\partial^2}{\partial x^2}[Dx^{2\gamma}w(x,t)]. \tag{3}$$

The probability density function (PDF) $w(x,t)$ and probability flux $\Pi(x,t)$ satisfy the following initial and boundary conditions

$$w(x,0) = \phi(x), \quad \Pi(0,t) = 0, \quad w(\infty,t) = 0. \tag{4}$$

Here, $\phi(x)$ is a non-negative function that satisfies the normalization condition and provides consistency of the initial and boundary conditions.

Introducing new variables $\xi = \beta(x^{1-\gamma} - \frac{a}{b})$, $\beta = \sqrt{\frac{b}{D(1-\gamma)}}$, and $\tau = (1-\gamma)bt$, we reduce Eq. (2) to

$$\frac{d\xi}{d\tau} = -\xi + \frac{\beta}{b}\zeta(\tau), \tag{2'}$$

where $\xi(\tau) \geqslant \xi_- = -\frac{\beta a}{b}$. The corresponding Fokker-Planck equation for the new PDF $w(\xi,\tau)$ is

$$\frac{\partial w(\xi,\tau)}{\partial \tau} = \frac{\partial^2 w(\xi,\tau)}{\partial \xi^2} + \frac{\partial}{\partial \xi}[\xi w(\xi,\tau)] \tag{3'}$$

with initial and boundary conditions

$$w(\xi,0) = \chi(\xi) \equiv \frac{\phi(x(\xi))}{1-\gamma}\beta^{\frac{1}{\gamma-1}}(\xi-\xi_-)^{\frac{\gamma}{1-\gamma}}, \quad \Pi(\xi_-,\tau) = 0, \quad w(\infty,\tau) = 0. \tag{4'}$$

The solution to problem (3′)–(4′) can be expressed in the form

$$w(\xi,\tau) = \int_{\xi_-}^{\infty} G(\xi,\tau,\xi',0)\chi(\xi')d\xi'. \tag{5}$$

Here, $G(\xi,\tau,\xi',\tau')$ is the Green's function for our problem. The function $G(\xi,\xi',\tau) \equiv G(\xi,\tau,\xi',0)$ can be found as a solution to the equation

$$\frac{\partial G}{\partial \tau} = \frac{\partial^2 G}{\partial \xi^2} + \frac{\partial}{\partial \xi}(\xi G), \tag{6}$$

with initial and boundary conditions

$$G(\xi,\xi',0) = \delta(\xi-\xi'), \quad \frac{\partial G}{\partial \xi} + \xi G|_{\xi=\xi_-} = 0, \quad |G| < \infty, \quad \tau > 0. \tag{7}$$

We solve the problem (6)–(7) using the Laplace transform

$$p\bar{G} - \delta(\xi-\xi') = \frac{\partial^2 \bar{G}}{\partial \xi^2} + \frac{\partial}{\partial \xi}(\xi\bar{G}), \tag{8}$$

$$\frac{\partial \bar{G}}{\partial \xi} + \xi\bar{G}|_{\xi=\xi_-} = 0, \quad |\bar{G}| < \infty. \tag{9}$$

Here, the bar denotes the transform

$$\bar{G}(\xi,\xi',p) = \int_0^{\infty} e^{-p\tau}G(\xi,\xi',\tau)d\tau. \tag{10}$$

For each subdomain $\xi < \xi'$ and $\xi' > \xi$, the substitution $\bar{G} = u(\xi)e^{-\xi^2/4}$ reduces Eq. (8) to the Weber equation, and therefore the solution to Eq. (8) is a superposition of the linearly independent combinations $e^{-\xi^2/4}D_{-p}(\xi)$ and $e^{-\xi^2/4}D_{-p}(-\xi)$, with $p > 0$. Here, $D_{-p}(\xi)$ is the parabolic cylinder function. Using the boundary conditions (9), we

have

$$\bar{G}(\xi,\xi',p)=\begin{cases}A(p)e^{-\xi^2/4}(D_{-p}(\xi)D_{-p-1}(-\xi_-)+D_{-p}(-\xi)D_{-p-1}(\xi_-)), & \xi<\xi',\\ B(p)e^{-\xi^2/4}D_{-p}(\xi), & \xi>\xi'.\end{cases} \tag{11}$$

One of the unknown functions $A(p)$ and $B(p)$ can be obtained using the continuity of the Green's function at $\xi=\xi'$. To get the second one, we integrate Eq. (8) across the discontinuity at ξ' to obtain the joining condition

$$\left.\frac{\partial\bar{G}}{\partial\xi}\right|_{\xi=\xi'+0}-\left.\frac{\partial\bar{G}}{\partial\xi}\right|_{\xi=\xi'-0}=-1.$$

Using [27], after some algebraic manipulations, we obtain the Green's function transform

$$\bar{G}(\xi,\xi',p)=e^{-(\xi^2-\xi'^2)/4}\frac{\Gamma(p)}{\sqrt{2\pi}}\begin{cases}\left(D_{-p}(\xi)D_{-p}(\xi')\frac{D_{-p-1}(-\xi_-)}{D_{-p-1}(\xi_-)}+D_{-p}(-\xi)D_{-p}(\xi')\right), & \xi<\xi',\\ \left(D_{-p}(\xi)D_{-p}(\xi')\frac{D_{-p-1}(-\xi_-)}{D_{-p-1}(\xi_-)}+D_{-p}(\xi)D_{-p}(-\xi')\right), & \xi>\xi',\end{cases} \tag{12}$$

or in more compact form

$$\bar{G}(\xi,\xi',p)=e^{-(\xi^2-\xi'^2)/4}\frac{\Gamma(p)}{\sqrt{2\pi}}\left(D_{-p}(\xi)D_{-p}(\xi')\frac{D_{-p-1}(-\xi_-)}{D_{-p-1}(\xi_-)}+H(\xi'-\xi)D_{-p}(-\xi)D_{-p}(\xi')+H(\xi-\xi')D_{-p}(-\xi')D_{-p}(\xi)\right), \tag{13}$$

where $H(x)$ is the Heaviside step function. Finally, applying the inverse Laplace transform, we obtain the desired distribution

$$w(\xi,\tau)=\int_{\xi_-}^{\infty}d\xi'\chi(\xi')\frac{1}{2\pi i}\int_{c-i\infty}^{c+i\infty}e^{p\tau}\bar{G}(\xi,\xi',p)dp, \tag{14}$$

where $c>0$. This is the Bromwich integral, which can be evaluated by means of the residue theorem.

1. Case of $\xi_-<0$

The Green's function transform (13) has two sets of simple poles:
(1) poles of $\Gamma(p)$, $p\in\mathbb{Z}^-$;
(2) roots p_k of the equation

$$D_{-p_k-1}(\xi_-)=0. \tag{15}$$

The real roots of Eq. (15) are negative. Dean [28] has demonstrated that the maximum root is $p_1<-1$ and $\lim_{\xi_-\to-\infty}p_k=-k$. Then, we get

$$w(\xi,\tau)=\sqrt{\frac{2}{\pi}}\frac{e^{-\xi^2/2}}{\operatorname{erfc}\left(\frac{\xi_-}{\sqrt{2}}\right)}+\frac{e^{-\xi^2/4}}{\sqrt{2\pi}}\sum_{k=1}^{\infty}\Gamma(p_k)D_{-p_k}(\xi)\frac{D_{-p_k-1}(-\xi_-)}{\frac{\partial}{\partial p}[D_{-p-1}(\xi_-)]_{p=p_k}}e^{p_k\tau}\int_{\xi_-}^{\infty}e^{\xi'^2/4}D_{-p_k}(\xi')\chi(\xi')d\xi', \tag{16}$$

where $\operatorname{erfc}(z)$ is the complementary error function. The expression for the derivative of the parabolic cylinder function is given in Appendix A.

Going back to the variable x, we obtain

$$w(x,t)=\sqrt{\frac{2}{\pi}}(1-\gamma)\beta x^{-\gamma}\left\{\frac{e^{-(\beta x^{1-\gamma}+\xi_-)^2/2}}{\operatorname{erfc}\left(\frac{\xi_-}{\sqrt{2}}\right)}+\frac{e^{-(\beta x^{1-\gamma}+\xi_-)^2/4}}{2}\sum_{k=1}^{\infty}\Gamma(p_k)D_{-p_k}(\beta x^{1-\gamma}+\xi_-)\frac{D_{-p_k-1}(-\xi_-)}{\frac{\partial}{\partial p}[D_{-p-1}(\xi_-)]_{p=p_k}}\right.$$
$$\left.\times\, e^{p_kb(1-\gamma)t}\int_0^{\infty}e^{(\beta x'^{1-\gamma}+\xi_-)^2/4}D_{-p_k}(\beta x'^{1-\gamma}+\xi_-)\phi(x')dx'\right\}. \tag{17}$$

Let us derive an analytical expression for the moments of x. Using [29] and the integral from Appendix B, we get

$$\mu_n(t)=\sqrt{\frac{2}{\pi}}e^{-\xi_-^2/4}\beta^{-\frac{n}{1-\gamma}}\Gamma\left(\frac{n}{1-\gamma}+1\right)\left\{\frac{D_{-\frac{n}{1-\gamma}-1}(\xi_-)}{\operatorname{erfc}\left(\frac{\xi_-}{\sqrt{2}}\right)}+\frac{1}{2}\sum_{k=1}^{\infty}\Gamma(p_k)D_{-\frac{n}{1-\gamma}-1-p_k}(\xi_-)\frac{D_{-p_k-1}(-\xi_-)}{\frac{\partial}{\partial p}[D_{-p-1}(\xi_-)]_{p=p_k}}\right.$$
$$\left.\times\, e^{p_kb(1-\gamma)t}\int_0^{\infty}e^{(\beta x'^{1-\gamma}+\xi_-)^2/4}D_{-p_k}(\beta x'^{1-\gamma}+\xi_-)\phi(x')dx'\right\}. \tag{18}$$

For sufficiently large times ($t \gg 1/[b(1-\gamma)]$) the PDF, given in Eq. (17) tends to the stationary distribution

$$w_{\rm st}(x) = \sqrt{\frac{2}{\pi}}(1-\gamma)\beta x^{-\gamma}\frac{e^{-(\beta x^{1-\gamma}+\xi_-)^2/2}}{\operatorname{erfc}\left(\frac{\xi_-}{\sqrt{2}}\right)}, \tag{19}$$

which is independent of the initial distribution. Then, the stationary moments of x are

$$\mu_n = \sqrt{\frac{2}{\pi}}\frac{e^{-\xi_-^2/4}}{\operatorname{erfc}\left(\frac{\xi_-}{\sqrt{2}}\right)}\left(\frac{D}{2b}\right)^n \Gamma(2n+1)D_{-2n-1}(\xi_-). \tag{20}$$

For $\gamma = 1/2$, we get

$$\langle x\rangle = \frac{a^2}{b^2} + \frac{D}{2b} + \frac{a}{b}\sqrt{\frac{D}{\pi b}}\frac{e^{-\frac{a^2}{bD}}}{\operatorname{erfc}\left(-\frac{a}{\sqrt{bD}}\right)}. \tag{21}$$

2. *Case of* $\xi_- = 0$

In this case, we can simplify Eq. (13), obtaining

$$\bar{G}(\xi,\xi',p) = e^{-(\xi^2-\xi'^2)/4}\frac{\Gamma(p)}{\sqrt{2\pi}}(D_{-p}(\xi)D_{-p}(\xi') + H(\xi'-\xi)D_{-p}(-\xi)D_{-p}(\xi') + H(\xi-\xi')D_{-p}(-\xi')D_{-p}(\xi)). \tag{22}$$

The Green's function transform (22) has simple poles $p \in \mathbb{Z}^-$. Then, we obtain

$$G(\xi,\xi',\tau) = e^{-(\xi^2-\xi'^2)/4}\sqrt{\frac{2}{\pi}}\sum_{n=0}^{\infty}\frac{D_{2n}(\xi)D_{2n}(\xi')}{(2n)!}e^{-2n\tau}. \tag{23}$$

Using the relationship between the parabolic cylinder functions and the Hermite polynomials [27], the series can be summed [30]:

$$G(\xi,\xi',\tau) = \sqrt{\frac{2}{\pi}}e^{-\xi^2/2}\frac{e^{\tau/2}}{\sqrt{2\sinh\tau}}\exp\left(-e^{-\tau}\frac{\xi^2+\xi'^2}{4\sinh\tau}\right)\cosh\left(\frac{\xi\xi'}{2\sinh\tau}\right), \quad \tau > 0. \tag{24}$$

Going back to the variable x, we get

$$w(x,t) = \sqrt{\frac{2}{\pi}}(1-\gamma)\beta x^{-\gamma}e^{-\beta^2x^{2-2\gamma}/2}\frac{e^{b(1-\gamma)t/2}}{\sqrt{2\sinh[b(1-\gamma)t]}}\int_0^\infty \exp\left(-e^{-b(1-\gamma)t}\beta^2\frac{x^{2-2\gamma}+x'^{2-2\gamma}}{4\sinh[b(1-\gamma)t]}\right)$$
$$\times \cosh\left(\frac{\beta^2(xx')^{1-\gamma}}{2\sinh[b(1-\gamma)t]}\right)\phi(x')dx'. \tag{25}$$

Using [29], we obtain expression for the moments of x

$$\mu_n(t) = \frac{1}{\sqrt{2\pi}}\left(\frac{e^{b(1-\gamma)t}}{2\sinh[b(1-\gamma)t]}\right)^{-\frac{n}{2-2\gamma}}\beta^{-\frac{n}{1-\gamma}}\Gamma\left(\frac{n}{1-\gamma}+1\right)\int_0^\infty \exp\left(-e^{-b(1-\gamma)t}\frac{\beta^2x'^{2-2\gamma}}{8\sinh[b(1-\gamma)t]}\right)$$
$$\times\left[D_{-\frac{n}{1-\gamma}-1}\left(\frac{\beta x'^{1-\gamma}e^{-b(1-\gamma)t/2}}{\sqrt{2\sinh[b(1-\gamma)t]}}\right) + D_{-\frac{n}{1-\gamma}-1}\left(-\frac{\beta x'^{1-\gamma}e^{-b(1-\gamma)t/2}}{\sqrt{2\sinh[b(1-\gamma)t]}}\right)\right]\phi(x')dx'. \tag{26}$$

For sufficiently large times ($t \gg 1/[b(1-\gamma)]$) the PDF (25) becomes the stationary distribution

$$w_{\rm st}(x) = \sqrt{\frac{2}{\pi}}(1-\gamma)\beta x^{-\gamma}e^{-\beta^2x^{2-2\gamma}/2}. \tag{27}$$

Then, the stationary moments of x are

$$\mu_n = \frac{1}{\sqrt{\pi}}\left(\frac{\sqrt{2}}{\beta}\right)^{\frac{n}{1-\gamma}}\Gamma\left(\frac{n}{2-2\gamma}+\frac{1}{2}\right). \tag{28}$$

It is easy to see that formulas (27) and (28) coincide with Eqs. (19) and (20) in the considered case. Moreover, Eq. (27) at $\gamma = 0$ is a semi-Gaussian distribution [1].

B. Poisson white pulse noise

In the previous section we examined the case of the white Gaussian noise. But for numerous applications it is more convenient to use pulse noise. Let us consider a stochastic process $\eta(t)$ consisting of delta pulses with constant magnitude f_0, which is suitable to be treated both analytically and numerically:

$$\eta(t) = f_0\sum_j \delta(t-t_j). \tag{29}$$

This noise source is characterized by a time interval between two successive pulses. We denote this interval as

$\vartheta_j = t_j - t_{j-1}$. This random quantity has a mean value which coincides with the quasiperiod of the process, i.e., $\langle\vartheta\rangle = T$.

The following question arises: are the results (17) and (18) still valid in the case of pulse noises? Let us consider the Langevin equation (1) with Poisson white noise source (i.e., ϑ has exponential distribution)

$$\frac{dx}{dt} = -bx + x^\gamma f_0 \sum_j \delta(t - t_j). \tag{30}$$

Using the variables $\xi = \sqrt{\frac{2}{(1-\gamma)bT}}(\frac{bT}{f_0}x^{1-\gamma} - 1)$ and $\tau = (1-\gamma)bt$, which coincide with the notations in Eq. (2′) with $D = f_0^2/2T$ and $a = f_0/T$, we can rewrite Eq. (30) as

$$\frac{d\xi}{d\tau} = -\xi - \sqrt{\frac{2}{(1-\gamma)bT}} + \sqrt{2(1-\gamma)bT}\sum_j \delta(\tau - \tau_j). \tag{30′}$$

The PDF $w(\xi,\tau)$ then obeys the equation [31]

$$\frac{\partial w(\xi,\tau)}{\partial\tau} = \frac{\partial}{\partial\xi}\left[\left(\xi + \sqrt{\frac{2}{(1-\gamma)bT}}\right)w(\xi,\tau)\right] + \frac{w(\xi - \sqrt{2(1-\gamma)bT},\tau) - w(\xi,\tau)}{(1-\gamma)bT}. \tag{31}$$

A Taylor series expansion of $w(\xi - \sqrt{2(1-\gamma)bT},\tau)$ with respect to the first argument around ξ gives

$$\frac{\partial w(\xi,\tau)}{\partial\tau} = \frac{\partial}{\partial\xi}[\xi w(\xi,\tau)] + \frac{\partial^2 w(\xi,\tau)}{\partial\xi^2} + 2\sum_{n=3}\frac{(-1)^n}{n!}[2(1-\gamma)bT]^{\frac{n}{2}-1}\frac{\partial^n w(\xi,\tau)}{\partial\xi^n}. \tag{31′}$$

It is easy to see that Eq. (31′) reduces to the Fokker-Planck equation (3′) when $(1-\gamma)bT \ll 1$. Keeping in Eq. (31′) the third derivative term and returning to variable x, we can obtain the stationary solution

$$w_{st}(x) = \mathcal{N}x^{-\gamma}e^{\frac{3}{2}\frac{x^{1-\gamma}}{(1-\gamma)f_0}}\,\mathrm{Ai}\left[\frac{\frac{6bTx^{1-\gamma}}{f_0} - \frac{15}{4}}{(6b(1-\gamma)T)^{\frac{2}{3}}}\right], \tag{32}$$

where $\mathrm{Ai}(z)$ is the Airy function.

For the Laplace transform with respect to ξ of the stationary solution to Eq. (31), we obtain

$$\bar{w}_{st}(p) = \int_0^\infty e^{-p\xi}w_{st}(\xi)d\xi = e^{-\frac{2}{bT}\mathrm{Ein}(f_0 p)}, \tag{33}$$

where $\mathrm{Ein}(z)$ is the modified exponential integral [32]. Then, the stationary moments of ξ are

$$\mu_n = (-1)^n\frac{d^n\bar{w}_{st}(p)}{dp^n}\bigg|_{p=0}. \tag{34}$$

For $\gamma = 1/2$, we get

$$\langle x\rangle = \frac{f_0^2}{b^2T^2} + \frac{f_0^2}{4bT}. \tag{35}$$

Comparing Eq. (35) with Eq. (21), we can see that in the case of the Gaussian white noise source we have an additional term, which is proportional to $w_{st}(\xi_-)$, due to the reflecting boundary condition at $\xi = \xi_-$ (or $x = 0$). Evidently, Eqs. (21) and (35) coincide (for appropriate choice of a and D), when $\xi_- \to -\infty$ or, equivalently, $bT \ll 1$.

III. THE EQUATION WITH CORRELATED PULSE NOISE

We characterize the properties of a noise source by its spectral density. In the general case, the spectral density for the process of Eq. (29) can be written as (see Appendix C)

$$S_\eta(\omega) = \frac{2f_0^2}{T}\left[1 + \sum_{m=1}^\infty \Theta_m(\omega) + \Theta_m(-\omega)\right], \tag{36}$$

where $\Theta_m(\omega)$ is a characteristic function of distribution of intervals between the nth and jth pulses with $m = n - j$.

Equation (2′) differs from well-known equation of a Ornstein-Uhlenbeck process only by the fact that $\xi \geqslant \xi_-$. We can analyze the possibility of neglecting this condition directly for white noise using the inequality $\sigma_{\xi W}^2 \ll \xi_-^2$, in asymptotics. Here $\sigma_{\xi W}^2$ is the variance of the white Gaussian noise. If the approximation of a linear filter can be applied for white noise, it can be applied for correlated noise, because usually its variance σ_ξ^2 is $\sigma_\xi^2 \leqslant \sigma_{\xi W}^2$.

Let us consider the case of $\gamma = 1/2$. We derive the following expression for the first moment of x:

$$\langle x\rangle = \frac{a^2}{b^2} + \frac{\langle\xi^2\rangle}{\beta^2}, \tag{37}$$

where $D = \int_0^\infty K_\zeta(t)dt$ in β, $\zeta(t) = \eta(t) - \langle\eta(t)\rangle$, and $a = \langle\eta(t)\rangle$.

Using the definition for the spectral density, we obtain for dimensionless time τ and frequency Ω

$$\langle\xi^2\rangle = K_\xi(0) = \frac{\beta^2}{4\pi b^2}\int_{-\infty}^\infty \frac{S'_\zeta(\Omega)d\Omega}{1+\Omega^2} = \frac{\beta^2}{b^2}\int_0^\infty e^{-\tau}K'_\zeta(\tau)d\tau. \tag{38}$$

Here, we use the following notations: $\tau = \frac{b}{2}t$, $K'_\zeta(\tau) = K_\zeta(t)$, $\Omega = \frac{2}{b}\omega$, and $S'_\zeta(\Omega) = \frac{b}{2}S_\zeta(\omega)$. Returning to time t instead of τ, we get the final expression for the mean value of x

$$\langle x\rangle = \frac{a^2}{b^2} + \frac{1}{2b}\int_0^\infty e^{-\frac{b}{2}t}K_\zeta(t)dt = \frac{a^2}{b^2} + \frac{\bar{K}_\zeta(\frac{b}{2})}{2b}, \tag{39}$$

where the bar denotes the Laplace transform.

For relatively small correlation time of noise $\tau_{cor} \ll 2/b$, we can simplify Eq. (39):

$$\langle x\rangle = \frac{a^2}{b^2} + \frac{1}{2b}\int_0^\infty K_\zeta(t)dt = \frac{a^2}{b^2} + \frac{S_\zeta(0)}{8b}. \tag{40}$$

Such an expression corresponds to the well-known approximation of a correlated process by using a Markov process [26]. For time intervals that are considerably greater than the correlation time, the process $\zeta(t)$ can be regarded as a Markov process. This means that the process $\zeta(t)$ with correlation functions $k_s(t_1,\ldots,t_s)$ can be replaced by a delta-correlated process, whose correlation functions are

$$K_s\delta(t_2 - t_1)\cdots\delta(t_s - t_1),$$

with the same intensity coefficients K_s as the actual process $\zeta(t)$.

Thus, the obtained Eq. (40) shows strong dependence of the mean solution to Eq. (1) on the correlation properties of the noise source considered.

Equation (40) is in full agreement with Eq. (35) in the case of Poisson white pulse noise, but it differs from Eq. (21) for a Gaussian white noise source by an additional term, which is proportional to $w_{st}(\xi_-)$. This difference can be eliminated if we take into account the reflection condition at the boundary in an additional term $-2\sum_{0<s\leqslant t}\dot{\xi}(s-0)\mathbb{1}|_{\xi(s)=\xi_-}$ [33]. For pulse noise with positive magnitudes such a correction is not needed, since $\dot{\xi}(t)$ is non-negative at $\xi=\xi_-$.

We consider two different types of noise source in Eq. (1). The first is the dead-time-distorted Poisson pulse (DTDP) process [34], and the second is the pulse process with fixed time intervals (FTI) [35].

A. Dead-time-distorted Poisson pulse noise

The DTDP process is a renewal pulse process with a delay ϑ_0 after each pulse. During this dead-time period it is forbidden for a new pulse to occur. After this period, the probability per unit time p to have the next pulse is constant. The delay ϑ_0 becomes therefore the minimum time interval between two adjacent pulses, that is $\vartheta_j \geqslant \vartheta_0$. This process is suitable to obtain noise sources with varying degree of randomness, ranging from white noise ($\vartheta_0 = 0$) to quasiperiodical process ($\vartheta_0 \simeq T$) [23].

The PDF of random time distances ϑ between adjacent pulses is

$$w(\vartheta) = pe^{p(\vartheta_0-\vartheta)}, \tag{41}$$

where ϑ is distributed in the interval $[\vartheta_0,\infty)$. The first moment and variance of ϑ are correspondingly

$$\langle\vartheta\rangle = \vartheta_0 + \frac{1}{p}, \quad \sigma_\vartheta^2 = (T-\vartheta_0)^2. \tag{42}$$

We define the parameter of periodicity as a ratio ϑ_0/T. Panels (a), (b), and (c) of Fig. 1 show three realizations of the DTDP process obtained with different values of periodicity parameter.

As this process is renewed, the characteristic function of intervals ϑ has the property $\Theta_m(\omega) = \Theta^m(\omega)$, because different time intervals are independent. It is easy to see that $\Theta(\omega) = pe^{i\omega\vartheta_0}/(p-i\omega)$. Using Eq. (36), we obtain the spectral density for the DTDP pulse process (see Fig. 2)

$$S_\eta(\omega) = \frac{2f_0^2}{T}\frac{1-|\Theta(\omega)|^2}{|1-\Theta(\omega)|^2} + \frac{4\pi f_0^2\delta(\omega)}{T^2}. \tag{43}$$

Using the expansion of the characteristic function in terms of moments, we obtain the expression for the spectral density of $\zeta(t)$ at $\omega = 0$

$$S_\zeta(0) = \frac{2\sigma_\vartheta^2 f_0^2}{T^3}, \tag{44}$$

which decreases with the increase in ϑ_0/T. Therefore from Eq. (40), the more the process is correlated the less the steady value of the moment of x is.

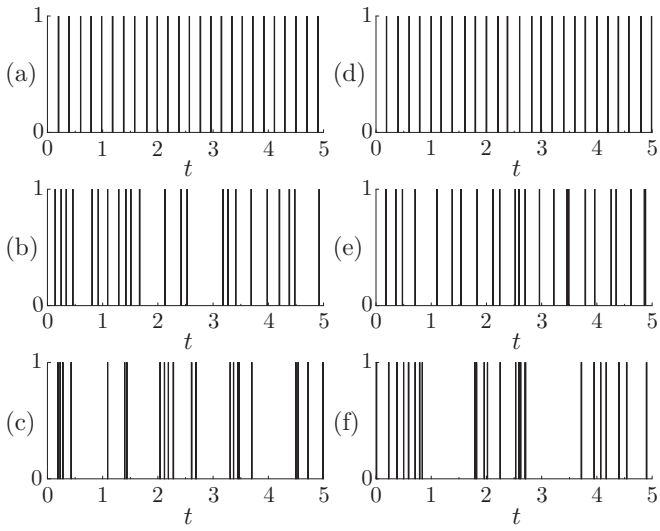

FIG. 1. DTDP process (left column) with $\vartheta_0/T = 0.9$ (a), 0.4 (b), 0 (c); and pulse process with FTI (right column) with $\vartheta_T/T = 0.05$ (d), 0.3 (e), 4.9 (f); $T = 0.2$, $f_0 = 1$. The mean value $\langle\vartheta\rangle$ is the same for all processes. Distribution of intervals between adjacent pulses has the same variance for the processes in the same row.

The correlation function can written as [23]

$$K_\zeta(t) = \frac{f_0^2}{T}\left[\delta(t) + \sum_{n=1}^{\infty}\frac{p^n(|t|-n\vartheta_0)^{n-1}}{(n-1)!} \times e^{-p(|t|-n\vartheta_0)}H(|t|-n\vartheta_0) - \frac{1}{T}\right], \tag{45}$$

where $H(x)$ is the Heaviside step function. Figure 3 shows that the correlation time of DTDP noise decreases with the decrease in ϑ_0/T.

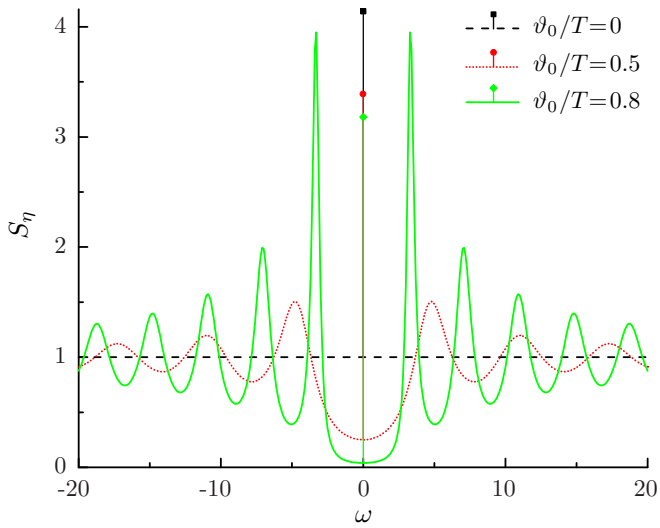

FIG. 2. (Color online) Spectral density of the DTDP process for different values of the periodicity parameter ($T = 2$, $f_0 = 1$): $\vartheta_0/T = 0.8$ (solid green line and diamonds), $\vartheta_0/T = 0.5$ (dotted red line and circles), $\vartheta_0/T = 0$ (dashed black line and squares). Vertical bars with top symbols represent the discrete parts of spectral density, whose values correspond to the delta function magnitudes.

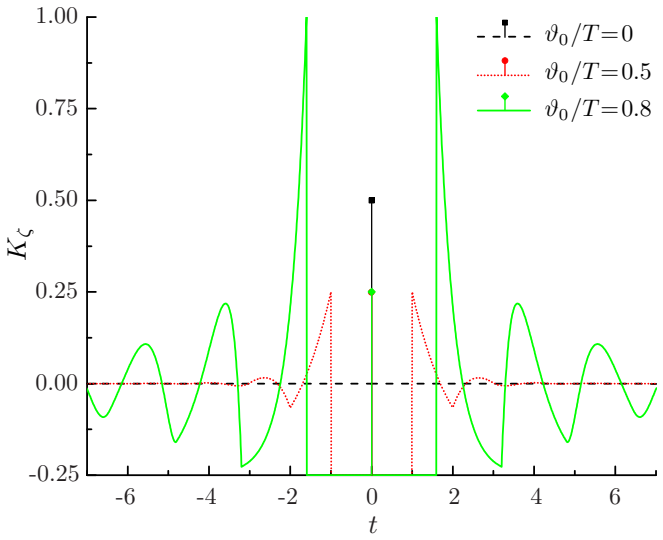

FIG. 3. (Color online) Correlation function of the DTDP process for different values of the periodicity parameter ($T = 2$, $f_0 = 1$): $\vartheta_0/T = 0.8$ (solid green line and diamonds), $\vartheta_0/T = 0.5$ (dotted red line and circles), $\vartheta_0/T = 0$ (dashed black line and squares). Vertical bars with top symbols represent the discrete parts of the correlation functions, whose values correspond to the delta function magnitudes. Note that the discrete parts overlap for $\vartheta_0/T = 0.8$ and $\vartheta_0/T = 0.5$.

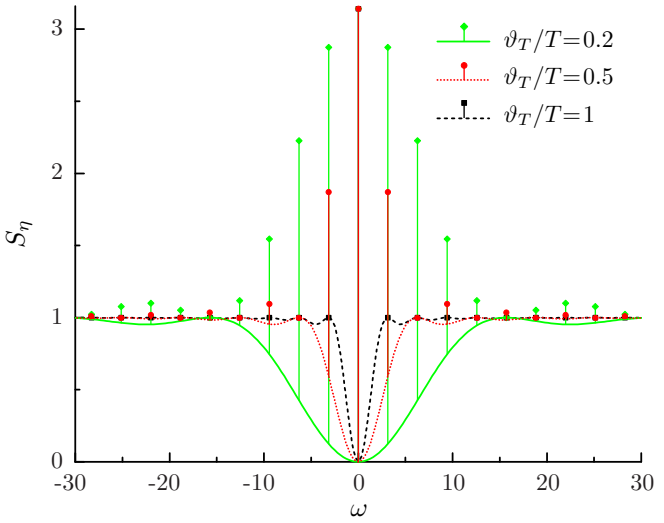

FIG. 4. (Color online) Spectral density of the FTI process for different values of interval ϑ_T ($T = 2$, $f_0 = 1$): $\vartheta_T/T = 0.2$ (solid green line and diamonds), $\vartheta_T/T = 0.5$ (dotted red line and circles), $\vartheta_T/T = 1$ (dashed black line and squares). Vertical bars with top symbols represent the discrete parts of spectral density, whose values correspond to the delta function magnitudes.

B. Pulse process with fixed time intervals

The FTI pulse process can be shown starting from periodically located points on the time axis with equal distance T between adjacent points. Each pulse of the sequence corresponds to one of these points and appears in the neighborhood of one of these points and at distance ν_n from it, where ν_n is a random value with zero mean and characteristic function $\Theta_\nu(\omega)$. Therefore the nth pulse occurrs at time $t_n = nT + \nu_n$. The pulse process (29) is characterized by the probability distribution of ν, and the characteristic function of time distance between nth and jth pulses is $\Theta_m(\omega) = e^{-i\omega mT}|\Theta_\nu(\omega)|^2$, $m = n - j$.

We consider the uniform PDF of the pulse position inside some interval with length $\vartheta_T \leqslant T$,

$$w(\nu) = \frac{1}{\vartheta_T}, \quad |\nu| \leqslant \frac{\vartheta_T}{2}, \tag{46}$$

and $\Theta_\nu(\omega) = \mathrm{sinc}(\omega\vartheta_T/2)$.

Probability distribution of intervals ϑ between two adjacent pulses is described by the expression

$$w(\vartheta) = \frac{\vartheta_T - |\vartheta - T|}{\vartheta_T^2}, \quad |\vartheta - T| \leqslant \vartheta_T. \tag{47}$$

We can derive the expressions for the mean and variance of the intervals between adjacent pulses:

$$\langle\vartheta\rangle = T, \quad \sigma_\vartheta^2 = \frac{\vartheta_T^2}{6}. \tag{48}$$

This process can be used to obtain noise sources with varying degree of randomness. Panels (d), (e), (f) of Fig. 1 present the process at different values of ϑ_T/T. We can see that this process looks like the DTDP process with the same characteristics of intervals. However, we will show that the correlation properties and the influence on the Langevin equation solution are different for these processes.

From Eq. (36) we obtain the spectral density of the noise under consideration:

$$S_\eta(\omega) = \frac{2f_0^2}{T}\Bigg[1 - |\Theta_\nu(\omega)|^2 + \frac{2\pi}{T}|\Theta_\nu(\omega)|^2 \sum_{n=-\infty}^{\infty} \delta\left(\omega - \frac{2\pi n}{T}\right)\Bigg]. \tag{49}$$

The spectral density consists of the Dirac comb or the Shah function $\mathrm{III}(\frac{\omega T}{2\pi})$ (discrete part) and continuous part (see Fig. 4). It is worth mentioning that $S_\zeta(0) = 0$ for any correlations of this noise.

The correlation function is obtained as

$$K_\zeta(t) = \frac{f_0^2}{T}\left[\delta(t) + \frac{1}{\vartheta_T}\sum_{\substack{n=-\infty \\ n\neq 0}}^{\infty} \Lambda\left(\frac{t - nT}{\vartheta_T}\right) - \frac{1}{T}\right], \tag{50}$$

where $\Lambda(x)$ is the triangle function. Figure 5 shows that the correlation time is infinite for all cases except $\vartheta_T/T = 1$.

IV. RESULTS AND DISCUSSION

As mentioned above, for sufficiently large times ($t \gg 1/[b(1-\gamma)]$) the PDF (17) becomes the stationary distribution (19). Figure 6 shows the relaxation of the different initial distributions $w(x,0)$, namely a delta function $w_d(x,0)$, uniform

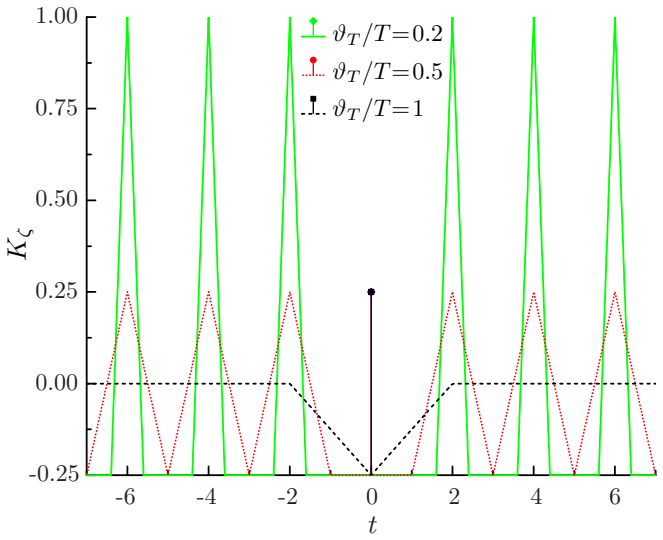

FIG. 5. (Color online) Correlation function of the FTI process for different values of interval ϑ_T ($T = 2$, $f_0 = 1$): $\vartheta_T/T = 0.2$ (solid green line and diamonds), $\vartheta_T/T = 0.5$ (dotted red line and circles), $\vartheta_T/T = 1$ (dashed black line and squares). Vertical bars with top symbols represent discrete parts of the correlation functions, whose values correspond to the delta function magnitudes. Note that discrete parts overlap for all three cases.

$w_u(x,0)$, and truncated binormal $w_b(x,0)$,

$$w_d(x,0) = \delta(x - x_0), \quad w_u(x,0) = \frac{1}{h}, \quad x \in [0,h],$$

$$w_b(x,0) = \frac{\kappa_1 \exp\left(-\frac{(x-\mu_1)^2}{2\sigma_1^2}\right)}{\sqrt{2\pi}\sigma_1\left[1 - \frac{1}{2}\operatorname{erfc}\left(\frac{\mu_1}{\sqrt{2}\sigma_1}\right)\right]} + \frac{\kappa_2 \exp\left(-\frac{(x-\mu_2)^2}{2\sigma_2^2}\right)}{\sqrt{2\pi}\sigma_2\left[1 - \frac{1}{2}\operatorname{erfc}\left(\frac{\mu_2}{\sqrt{2}\sigma_2}\right)\right]}, \quad x \geqslant 0, \quad (51)$$

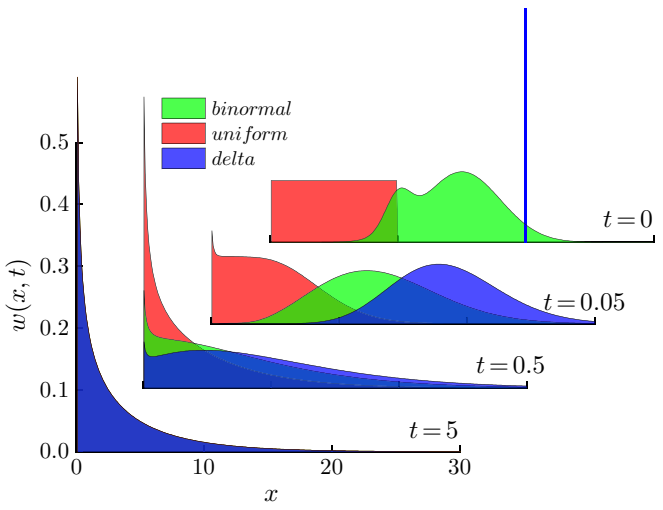

FIG. 6. (Color online) Time evolution of various initial distributions from Eq. (51): truncated binormal (green [light gray] area), uniform (red [gray] area), and delta function (blue [dark gray] area). The parameter values are $\gamma = 1/2$, $b = 2$, $a = 1$, $D = 10$.

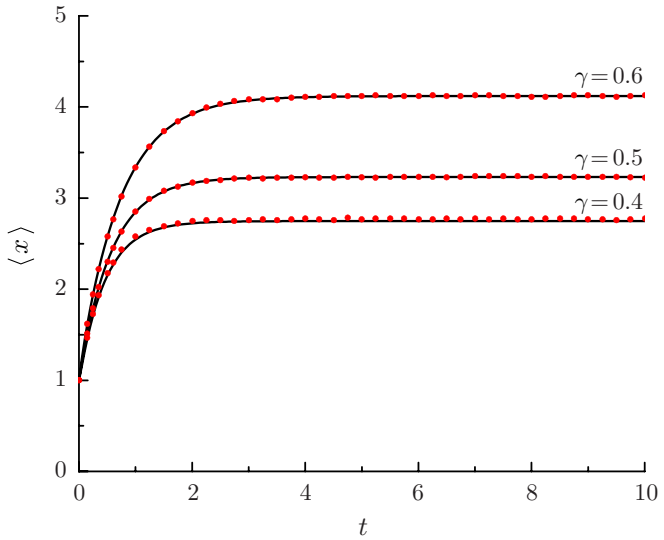

FIG. 7. (Color online) Plot of mean x vs time for different values of γ and fixed values of other parameters: $a = 1$, $b = 2$, $D = 10$. Analytical (solid lines) and numerical (dots) results, obtained using a Gaussian white noise source, are compared.

to the stationary distribution (19). Here $x_0 = 20$, $h = 10$, $\kappa_1 = 1/7$, $\mu_1 = 10$, $\sigma_1 = 1$, $\kappa_2 = 6/7$, $\mu_2 = 15$, and $\sigma_2 = 3$.

Here, we present results obtained by numerical integration of Eq. (1). Three kinds of noise were used in our calculations: Gaussian white noise with nonzero mean; DTDP pulse noise with delay ϑ_0 and mean interval between adjacent pulses T; FTI pulse noise described by fixed time interval T and interval ϑ_T inside which the pulse can appear.

We use the order 1.5 strong Taylor scheme [36] with a timestep of 10^{-6} for simulation of Eq. (1) with Gaussian white noise and direct simulation for DTDP and FTI noise. The Mersenne twister [37] is used as pseudorandom number generator. The numerical results are averaged over 1 000 000 realizations.

Figures 7 and 8 show the mean and the variance as the results of numerical integration and the analytical solution to Eq. (18) in the presence of a source of Gaussian white noise for different values of γ. Here, for the other parameter values we set $a = 1, b = 2, D = 10$ and delta-function initial distribution with $x_0 = 1$. Clearly, the analytical and numerical results are in agreement.

Figures 9 and 10 also present the results of numerical and analytical solutions in the presence of a source of Gaussian white noise for $\gamma = 1/2$ and the Rayleigh initial distribution with $\sigma = 2$. Here, we use the following sets of parameter values: $a = 1$, $b = 2$, $D = 10$; $a = 4$, $b = 2$, $D = 3$; $a = 2$, $b = 3$, $D = 5$.

Let us compare the analytical expressions (20), (32), and (35), when the condition $(1 - \gamma)bT \ll 1$ is not satisfied. We use $f_0 = 1$, $T = 0.7$, $b = 1$, and $\gamma = 1/2$. Figure 11 clearly shows that the analytical result (35) is in good agreement with the numerical simulation of Eq. (30), whereas formula (20) overestimates quantity $\langle x \rangle$ and Eq. (32) underestimates it.

Figure 12 shows the results of numerical simulations with DTDP and FTI noises and analytical stationary solution using

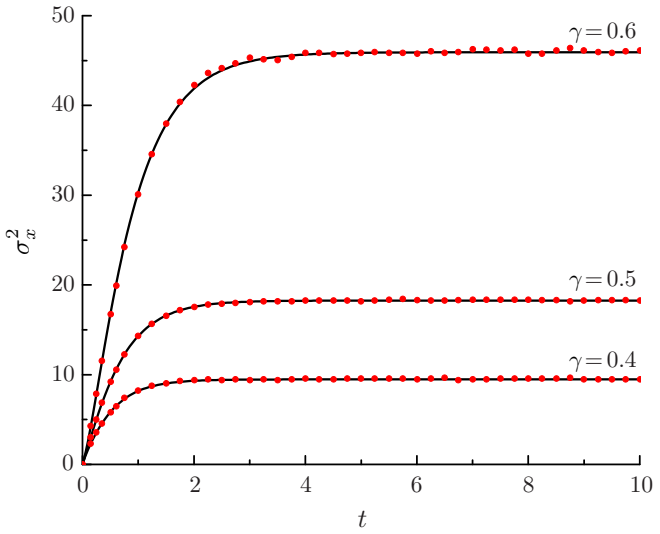

FIG. 8. (Color online) Plot of the variance of x vs time for different values of γ and fixed values of other parameters: $a = 1$, $b = 2$, $D = 10$. Analytical (solid lines) and numerical (dots) results, obtained using a Gaussian white noise source, are compared.

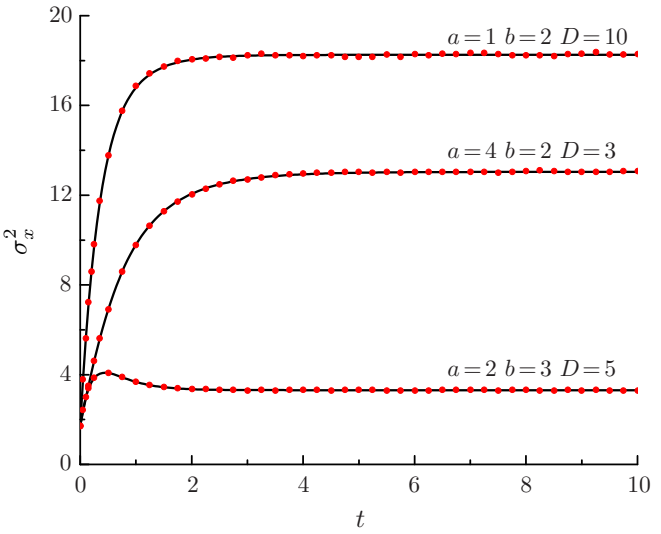

FIG. 10. (Color online) Plot of the variance of x vs time for different values of a, b, D, and a fixed value of the exponent $\gamma = 1/2$. Analytical (solid lines) and numerical (dots) results, obtained using a Gaussian white noise source, are compared.

Eq. (20). Here, we use the parameters $\gamma = 1/2$, $f_0 = 1$, $b = 0.1$, $T = 0.1$, and the Rayleigh initial distribution with $\sigma = 1$. We choose ϑ_0 and ϑ_T, so that the variances of delay between adjacent pulses are equal for both kinds of noise: high periodicity limit $\sigma_\vartheta^2 = 10^{-6}$ ($\vartheta_0/T = 0.99$ and $\vartheta_T/T = 0.024$) and low periodicity limit $\sigma_\vartheta^2 = 0.00167$ ($\vartheta_0/T = 0.59$ and $\vartheta_T/T = 1$). Certainly, the mean distance between adjacent pulses is the same, $\langle\vartheta\rangle = T$. For the analytical solution we use $a = f_0/T$ and $D = S_\zeta(0)/4$ for corresponding noises. Clearly, the analytical and numerical results are in good agreement. We note that in Figs. 11 and 12 the scale of the y axis is chosen so that the differences in mean values, obtained using Eqs. (20), (32), and (35) for Fig. 11 and Eq. (20) for Fig. 12, are noticeable. This allows to highlight the differences in mean values due to different statistical properties of the noise source. However, the deviations from analytical results are not as large as it might seem at a first glance. In Fig. 11 indeed the standard deviation of mean value, defined as $\sigma_{\langle x\rangle} = \sigma_x/\sqrt{N}$, is about 0.002 (0.08%). In Fig. 12 the standard deviation of mean value is 0.4 (0.004%) for DTDP noise with $\vartheta_0/T = 0.59$. For DTDP noise with $\vartheta_0/T = 0.99$ and FTI noises this value is much smaller: 0.01 and 0 [from Eq. (49)], respectively. As a conclusion, these deviations are comparable with results presented in other figures, such as Fig. 9 where the standard

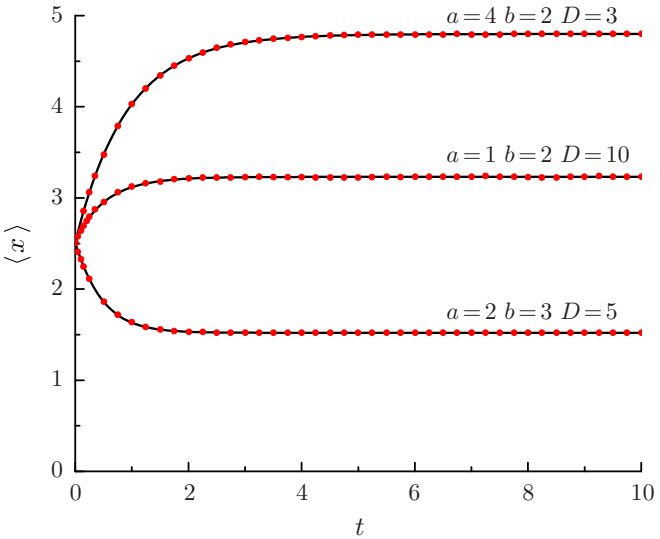

FIG. 9. (Color online) Plot of mean x vss time for different values of the a, b, D, and a fixed value of the exponent $\gamma = 1/2$. Analytical (solid lines) and numerical (dots) results, obtained using a Gaussian white noise source, are compared.

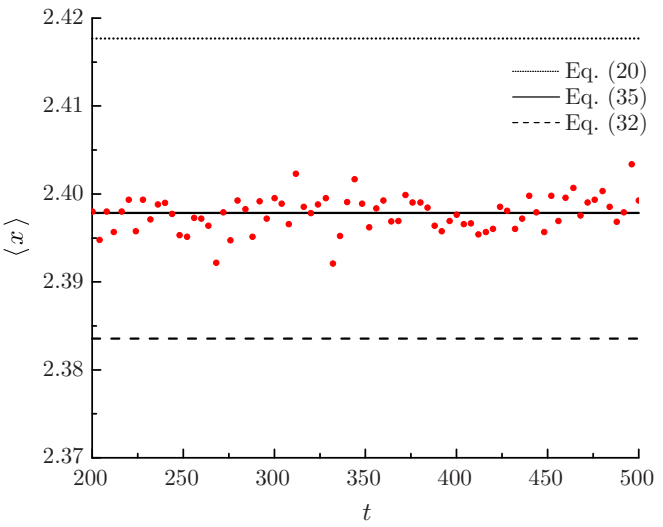

FIG. 11. (Color online) Plot of mean x vs time for Poisson white pulse noise (circles) and derived from stationary solutions: (solid line) Eq. (35), (dashed line) Eq. (32), and (dotted line) Eq. (20). The values of the parameters are $\gamma = 1/2$, $b = 1$, $T = 0.7$, $f_0 = 1$.

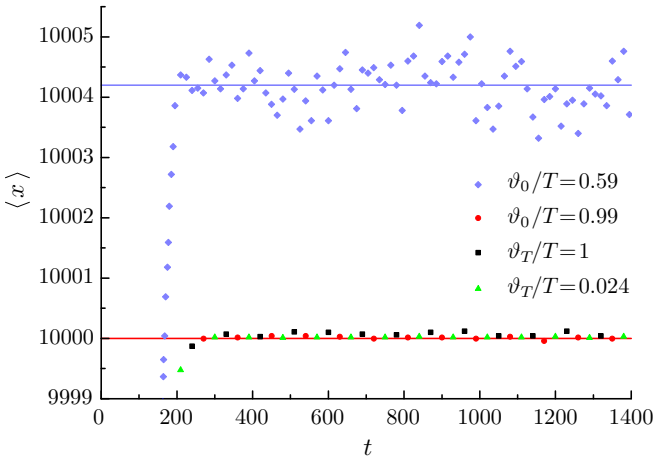

FIG. 12. (Color online) Plot of mean x vs time: DTDP noise for different values of ϑ_0, namely $\vartheta_0/T = 0.59$ (violet diamonds) and $\vartheta_0/T = 0.99$ (red circles); FTI noise for different values of ϑ_T, namely $\vartheta_T/T = 1$ (black squares) and $\vartheta_T/T = 0.024$ (green triangles). The values of the other parameters are $\gamma = 1/2$, $b = 0.1$, $T = 0.1$, $f_0 = 1$. Stationary analytical solution, obtained from Eq. (20) with $D = S_\zeta(0)/4$ for $\vartheta_0/T = 0.59$ (violet [gray] line), $\vartheta_0/T = 0.99$ and both FTI noises (red [dark gray] line).

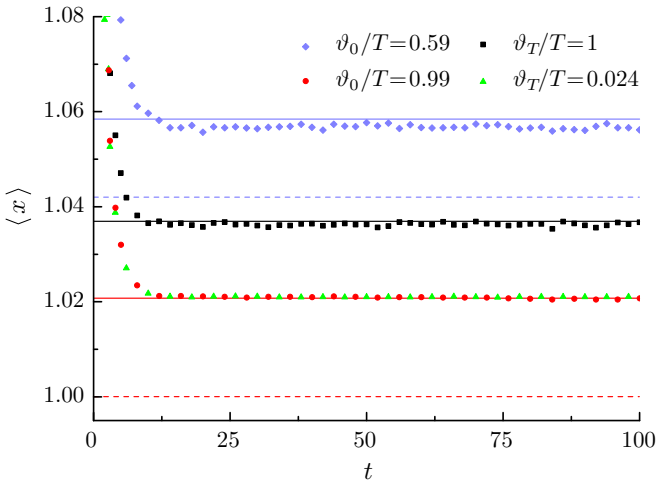

FIG. 13. (Color online) Plot of mean x vs time: DTDP noise for different values of ϑ_0, namely $\vartheta_0/T = 0.59$ (violet diamonds) and $\vartheta_0/T = 0.99$ (red circles); FTI noise for different values of ϑ_T, namely $\vartheta_T/T = 1$ (black squares) and $\vartheta_T/T = 0.024$ (green triangles). The values of the other parameters are $\gamma = 1/2$, $b = 1$, $T = 1$, $f_0 = 1$. Stationary analytical solution, obtained from Eq. (20) with $D = \bar{K}_\zeta(b/2)$ for $\vartheta_0/T = 0.59$ (solid violet [gray] line), $\vartheta_T/T = 1$ (solid black line), $\vartheta_0/T = 0.99$, and $\vartheta_T/T = 0.024$ (solid red [dark gray] line); and with $D = S_\zeta(0)/4$ for $\vartheta_0/T = 0.59$ (dashed violet [gray] line), $\vartheta_0/T = 0.99$ and both FTI noises (dashed red [dark gray] line).

deviation is about 0.07% for parameter values $a = 4$, $b = 2$, and $D = 3$. The results shown in Fig. 12 indicate that in the case of DTDP noise the growth of the periodicity parameter, which corresponds to the increase of the delay, reduces the intensity of the fluctuations in the mean solution to Eq. (1). Conversely, less regular noise causes higher saturation level and larger fluctuations in the solutions. In contrast, in the case of the FTI noise the change of periodicity does not influence the saturation level of the solution.

The difference between the numerical solutions to Eq. (1) with FTI noise having different σ_ϑ^2 is not necessarily negligible. Figure 13 illustrates this fact for the parameters $\gamma = 1/2$, $f_0 = 1$, $b = 1$, $T = 1$, and the Rayleigh initial distribution with $\sigma = 1$. Comparison of the results of numerical simulation and stationary analytical solutions, obtained from Eq. (20) with different approximations of value D from Eqs. (39) and (40) [$D = \bar{K}_\zeta(b/2)$ and $D = S_\zeta(0)/4$, respectively], shows that the statement $D = S_\zeta(0)/4$ became invalid for $(1-\gamma)bT \sim 1$. Now it is clear that the condition $(1-\gamma)bT \ll 1$ holds for parameters of Fig. 12, but it becomes invalid for parameters of Fig. 13.

Finally, we present the results of numerical simulations with DTDP and FTI noises and the analytical stationary solution using Eq. (20) for the case when γ is different from 1/2 (see Figs. 14 and 15). Here, we use the parameters $f_0 = 1$, $b = 0.5$, $T = 0.5$, and the delta-function initial distribution with $x_0 = 5$. Again, for the analytical solution we use $a = f_0/T$ and $D = S_\zeta(0)/4$. Note that the analytical and numerical results are in satisfactory agreement even in the case of $(1-\gamma)bT \lesssim 1$. The comparison of Figs. 14 and 15 demonstrates that the time of relaxation to the steady state increases with the increase of γ.

The Fokker-Planck equation allows us to follow the dynamics of the mean solution to Eq. (1); however, it can be

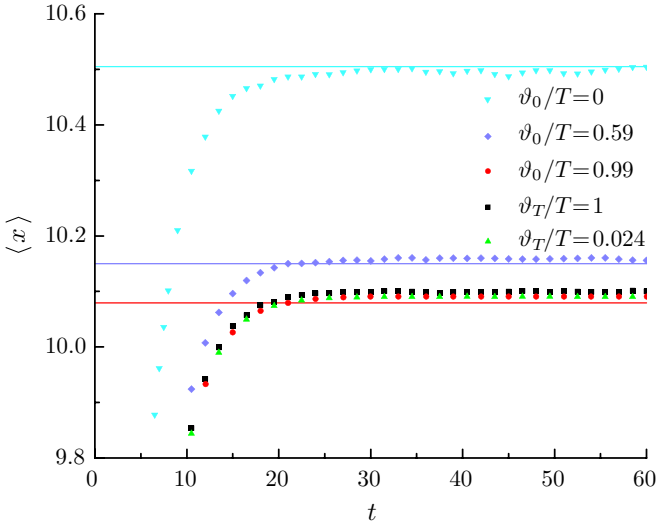

FIG. 14. (Color online) Plot of mean x vs time: DTDP noise for different values of ϑ_0, namely $\vartheta_0/T = 0$ (cyan down triangles), $\vartheta_0/T = 0.59$ (violet diamonds), $\vartheta_0/T = 0.99$ (red circles); FTI noise for different values of ϑ_T, namely $\vartheta_T/T = 1$ (black squares) and $\vartheta_T/T = 0.024$ (green up triangles). The values of the other parameters are $\gamma = 0.4$, $b = 0.5$, $T = 0.5$, $f_0 = 1$. Stationary analytical solution, obtained from Eq. (20) with $D = S_\zeta(0)/4$ for $\vartheta_0/T = 0$ (cyan [light gray] line), $\vartheta_0/T = 0.59$ (violet [gray] line), $\vartheta_0/T = 0.99$ and both FTI noises (red [dark gray] line).

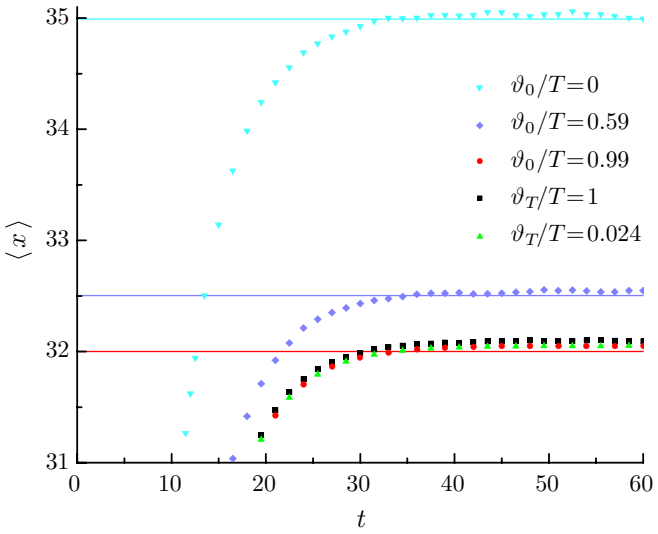

FIG. 15. (Color online) Plot of mean x vs time: DTDP noise for different values of ϑ_0, namely $\vartheta_0/T = 0$ (cyan down triangles), $\vartheta_0/T = 0.59$ (violet diamonds), $\vartheta_0/T = 0.99$ (red circles); FTI noise for different values of ϑ_T, namely $\vartheta_T/T = 1$ (black squares) and $\vartheta_T/T = 0.024$ (green up triangles). The values of the other parameters are $\gamma = 0.6$, $b = 0.5$, $T = 0.5$, $f_0 = 1$. Stationary analytical solution, obtained from Eq. (20) with $D = S_\xi(0)/4$ for $\vartheta_0/T = 0$ (cyan [light gray] line), $\vartheta_0/T = 0.59$ (violet [gray] line), $\vartheta_0/T = 0.99$ and both FTI noises (red [dark gray] line).

applied only in the case when the stochastic term is represented with the white noise. For the colored noises we can consider only the steady state.

V. SUMMARY

The problem of the relaxation dynamics to the steady state of a system under the influence of different kinds of multiplicative noise is well understood for two limit cases: the predominance of noise (thermal equilibrium) or, in contrast, the predominance of the deterministic term (small noise approximation). The correlation properties of noise are not significant for these limit cases. However, when noise and deterministic terms are equally important, the noise correlation properties affect not only the transient dynamics to the steady state, but also the values of the steady state moments of the system investigated.

We have considered a relatively simple Langevin equation, in which the random process x relaxes to a steady value. All characteristics of this process x, such as PDF and all moments, can be obtained only for white noise by solving Fokker-Planck equation. Under some conditions and at the steady state, the solution to the Fokker-Planck equation can be used also for correlated noise, provided that some transformation of the parameters is carried out. The spectrum density of the noise determines this transformation.

The main result of this investigation is that the higher the noise correlation is, the smaller the mean value of x is. We have considered noises with equal intensities and mean values but with different correlation properties. We have demonstrated that their contributions to the mean value of x vary for different noises. The observed dependence of the mean value of x on the spectrum density of the noise is in good agreement with the numerical calculations.

For the applications mentioned in Sec. I, we can say the following. From the point of view of the billiard theory, for scatterers of finite mass the final particle velocity is less for periodical motion than for random motion. The kinetic energy of a particle in a flow of independently moving particles is larger than for correlated ones. Periodical deposition of clusters on a surface is more appropriate for the case when the size of formed islands needs to be smaller. A population of predators is higher for random change of the prey population.

ACKNOWLEDGMENTS

We are very grateful to Andrey Chikishev for fruitful discussions. This work was supported by the Supercomputing Center of Lomonosov Moscow State University [38]. E.A., D.V., and B.S. acknowledge the financial support of the Ministero dell'Istruzione, dell'Università e della Ricerca (Italy).

APPENDIX A: DERIVATIVE OF THE PARABOLIC CYLINDER FUNCTION WITH RESPECT TO PARAMETER

We derive an expression for the derivative $\partial D_{-p-1}(z)/\partial p$ in a similar way as in Ref. [39]. The parabolic cylinder function can be represented in terms of the Kummer functions [27]:

$$D_{-p-1}(\xi_-) = 2^{-(p+1)/2} e^{-\xi_-^2/4} \left[\frac{\Gamma\left(\frac{1}{2}\right)}{\Gamma\left(\frac{p+2}{2}\right)} {}_1F_1\left(\frac{p+1}{2}, \frac{1}{2}, \frac{\xi_-^2}{2}\right) + \frac{\xi_-}{\sqrt{2}} \frac{\Gamma\left(-\frac{1}{2}\right)}{\Gamma\left(\frac{p+1}{2}\right)} {}_1F_1\left(\frac{p+2}{2}, \frac{3}{2}, \frac{\xi_-^2}{2}\right) \right]. \quad \text{(A1)}$$

Differentiating expression (A1) with respect to p and taking into account that the derivative of the confluent hypergeometric function with respect to the parameter can be expressed in terms of two-argument Kampé de Fériet–like hypergeometric functions $\Theta^{(1)}$ [40], we find with allowance for expression (15)

$$\left.\frac{\partial}{\partial p} D_{-p-1}(\xi_-)\right|_{p=p_k} = 2^{-(p_k+3)/2} e^{-\xi_-^2/4} \sqrt{\pi} \left\{ \frac{1}{\Gamma\left(\frac{p_k+2}{2}\right)} \left[\xi_-^2 \Theta^{(1)}\left(\begin{matrix} 1,1 \\ \frac{p_k+3}{2} \end{matrix} \middle| \begin{matrix} \frac{p_k+1}{2}, \frac{p_k+3}{2} \\ 2, \frac{3}{2} \end{matrix} \middle| \frac{\xi_-^2}{2}, \frac{\xi_-^2}{2} \right) - G(p_k+1)\, {}_1F_1\left(\frac{p_k+1}{2}, \frac{1}{2}, \frac{\xi_-^2}{2}\right) \right] - \frac{\sqrt{2}}{\Gamma\left(\frac{p_k+1}{2}\right)} \frac{\xi_-^3}{3} \Theta^{(1)}\left(\begin{matrix} 1,1 \\ \frac{p_k+4}{2} \end{matrix} \middle| \begin{matrix} \frac{p_k+2}{2}, \frac{p_k+4}{2} \\ 2, \frac{5}{2} \end{matrix} \middle| \frac{\xi_-^2}{2}, \frac{\xi_-^2}{2} \right) \right\}. \quad \text{(A2)}$$

Here, $G(z)$ is the Erdélyi G function [27].

APPENDIX B: COMPUTATION OF AN INTEGRAL CONTAINING THE PARABOLIC CYLINDER FUNCTION

We consider the integral

$$\int_0^\infty z^{\mu-1}e^{-(z+z_0)^2/4}D_\nu(z+z_0)dz, \quad \mathrm{Re}\,\mu > 0. \tag{B1}$$

Let us use the following integral representation for the parabolic cylinder function [32]:

$$D_\nu(z) = \frac{e^{z^2/4}}{\sqrt{2\pi}\,i}\int_{c-i\infty}^{c+i\infty} e^{-zt+\frac{1}{2}t^2}t^\nu dt, \quad |\arg t| < \pi/2,\ c > 0. \tag{B2}$$

Changing the order of integration and using [29], we get

$$\begin{aligned}&\int_0^\infty z^{\mu-1}e^{-(z+z_0)^2/4}D_\nu(z+z_0)dz\\ &= \frac{1}{\sqrt{2\pi}\,i}\int_{c-i\infty}^{c+i\infty} e^{-z_0t+\frac{1}{2}t^2}\left[\int_0^\infty z^{\mu-1}e^{-zt}dz\right]t^\nu dt\\ &= \frac{\Gamma(\mu)}{\sqrt{2\pi}\,i}\int_{c-i\infty}^{c+i\infty} e^{-z_0t+\frac{1}{2}t^2}t^{\nu-\mu}dt = \Gamma(\mu)e^{-z_0^2/4}D_{\nu-\mu}(z_0).\end{aligned} \tag{B3}$$

APPENDIX C: CALCULATION OF SPECTRAL DENSITY OF DELTA PULSES SEQUENCE

The derivation of the equations mentioned in this section was carried out in accordance with the algorithm suggested in [35]. Let us consider a pulsed stochastic process $\eta(t)$ consisting of $2N+1$ delta pulses, which can be represented by Eq. (29), where $j = [-N; N]$. $\mathcal{H}_N(\omega)$ is a Fourier transform of $\eta(t)$:

$$\mathcal{H}_N(\omega) = f_0\sum_{j=-N}^{N} e^{-i\omega t_j}, \tag{C1}$$

$$\begin{aligned}\langle|\mathcal{H}_N(\omega)|^2\rangle &= f_0^2\left\langle\sum_{n=-N}^{N}\sum_{j=-N}^{N} e^{-i\omega(t_n-t_j)}\right\rangle\\ &= f_0^2\sum_{n=-N}^{N}\sum_{j=-N}^{N}\Theta_{nj}(\omega)\\ &= f_0^2\left\{(2N+1)+\sum_{m=1}^{2N}(2N+1-m)\right.\\ &\quad\left.\times[\Theta_m(\omega)+\Theta_m(-\omega)]\right\}, \quad m = n-j,\end{aligned} \tag{C2}$$

where $\Theta_{nj}(\omega)$ is a characteristic function for the interval between nth and jth pulses.

Then, spectrum of pulsed process can be described as

$$\begin{aligned}S_\eta(\omega) &= \lim_{N\to\infty}\frac{2}{(2N+1)T}\langle|\mathcal{H}_N(\omega)|^2\rangle\\ &= \frac{2f_0^2}{T}\left[1+\sum_{m=1}^{\infty}\Theta_m(\omega)+\Theta_m(-\omega)\right],\end{aligned} \tag{C3}$$

when the series $\sum_{m=1}^{\infty}\Theta_m(\omega)$ converges [strictly speaking, the limit in Eq. (C3) may exists in some cases even if the series diverges].

[1] S. Ciuchi, F. de Pasquale, and B. Spagnolo, Nonlinear relaxation in the presence of an absorbing barrier, Phys. Rev. E **47**, 3915 (1993).

[2] M. A. Muñoz, Multiplicative noise in non-equilibrium phase transitions: A tutorial, in *Advances in Condensed Matter and Statistical Physics*, edited by E. Korutcheva and R. Cuerno (Nova Science Publishers, New York, 2004), pp. 37–68.

[3] A. A. Dubkov and B. Spagnolo, Acceleration of diffusion in randomly switching potential with supersymmetry, Phys. Rev. E **72**, 041104 (2005).

[4] M. A. Muñoz, F. Colaiori, and C. Castellano, Mean-field limit of systems with multiplicative noise, Phys. Rev. E **72**, 056102 (2005).

[5] S. Ciuchi, F. de Pasquale, and B. Spagnolo, Self-regulation mechanism of an ecosystem in a non-Gaussian fluctuation regime, Phys. Rev. E **54**, 706 (1996).

[6] D. Valenti, L. Schimansky-Geier, X. Sailer, and B. Spagnolo, Moment equations for a spatially extended system of two competing species, Eur. Phys. J. B **50**, 199 (2006).

[7] H. Hasegawa, Dynamics of the Langevin model subjected to colored noise: Functional-integral method, Physica A **387**, 2697 (2008).

[8] G. Bonanno, D. Valenti, and B. Spagnolo, Mean escape time in a system with stochastic volatility, Phys. Rev. E **75**, 016106 (2007).

[9] A. Fiasconaro, A. Ochab-Marcinek, B. Spagnolo, and E. Gudowska-Nowak, Monitoring noise-resonant effects in cancer growth influenced by external fluctuations and periodic treatment, Eur. Phys. J. B **65**, 435 (2008).

[10] A. Manor and N. M. Shnerb, Multiplicative Noise and Second Order Phase Transitions, Phys. Rev. Lett. **103**, 030601 (2009).

[11] P. L. Lions and A. S. Sznitman, Stochastic differential equations with reflecting boundary conditions, Commun. Pure Appl. Math. **37**, 511 (1984).

[12] A. Y. Loskutov, A. B. Ryabov, and L. G. Akinshin, Mechanism of Fermi acceleration in dispersing billiards with time-dependent boundaries, J. Exp. Theor. Phys. **89**, 966 (1999).

[13] A. Krasnova and O. Chichigina, Fermi acceleration as a possible mechanism of rapid diffusion of gold clusters on graphite, Moscow Univ. Phys. Bull. **67**, 48 (2012).

[14] T. Michely and J. Krug, *Islands, Mounds and Atoms* (Springer-Verlag, Berlin, 2004).

[15] A. Perez, P. Mélinon, V. Dupuis *et al.*, Functional nanostructures from clusters, Int. J. Nanotechnol. **7**, 523 (2010).

[16] P. Jensen and B. Niemeyer, The effect of a modulated flux on the growth of thin films, Surf. Sci. **384**, L823 (1997).

[17] E. I. Anashkina, O. A. Chichigina, D. Valenti, A. V. Kargovsky, and B. Spagnolo, Predator population depending on lemming cycles, Int. J. Mod. Phys. B **29**, 1541003 (2015).

[18] K. C. Chan, G. A. Karolyi, F. A. Longstaff, and A. B. Sanders, An empirical comparison of alternative models of the short-term interest rate, J. Finance **47**, 1209 (1992).

[19] D. Valenti, B. Spagnolo, and G. Bonanno, Hitting time distributions in financial markets, Physica A **382**, 311 (2007).

[20] J. Łuczka, T. Czernik, and P. Hänggi, Symmetric white noise can induce directed current in ratchets, Phys. Rev. E **56**, 3968 (1997).

[21] A. Porporato and P. D'Odorico, Phase Transitions Driven by State-Dependent Poisson Noise, Phys. Rev. Lett. **92**, 110601 (2004).

[22] Y. Wu and W. Q. Zhu, Stochastic analysis of a pulse-type prey-predator model, Phys. Rev. E **77**, 041911 (2008).

[23] O. A. Chichigina, A. A. Dubkov, D. Valenti, and B. Spagnolo, Stability in a system subject to noise with regulated periodicity, Phys. Rev. E **84**, 021134 (2011).

[24] A. V. Kargovsky, E. I. Anashkina, O. A. Chichigina, and A. K. Krasnova, Velocity distribution for quasistable acceleration in the presence of multiplicative noise, Phys. Rev. E **87**, 042133 (2013).

[25] D. Valenti, O. Chichigina, A. Dubkov, and B. Spagnolo, Stochastic acceleration in generalized squared Bessel processes, J. Stat. Mech. (2015) P02012.

[26] R. L. Stratonovich, *Topics in the Theory of Random Noise* (Gordon and Breach, New York, 1967).

[27] A. Erdélyi, W. Magnus, F. Oberhettinger, and F. G. Tricomi, *Higher Transcendental Functions* (McGraw-Hill, New York, 1953).

[28] P. Dean, The constrained quantum mechanical harmonic oscillator, Proc. Camb. Philos. Soc. **62**, 277 (1966).

[29] I. S. Gradshteyn and I. M. Ryzhik, *Table of Integrals, Series, and Products* (Elsevier/Academic Press, Amsterdam, 2007).

[30] Y. A. Brychkov, *Handbook of Special Functions: Derivatives, Integrals, Series and Other Formulas* (CRC Press, Boca Raton, 2008).

[31] M. Lax, Classical noise IV: Langevin methods, Rev. Mod. Phys. **38**, 541 (1966).

[32] M. Abramowitz and I. A. Stegun, *Handbook of Mathematical Functions with Formulas, Graphs, and Mathematical Tables* (Dover, New York, 1964).

[33] E. Jacob, A Langevin process reflected at a partially elastic boundary: I, Stochastic Process. Appl. **122**, 191 (2012).

[34] J. W. Müller, Some formulae for a dead-time-distorted poisson process: To André Allisy on the completion of his first half century, Nucl. Instrum. Methods **117**, 401 (1974).

[35] B. R. Levin, *Theoretical Principles of Statistical Radiophysics* (Radio and Communications, Moscow, 1989) (in Russian).

[36] P. E. Kloeden, E. Platen, and H. Schurz, *Numerical Solution of SDEs Through Computer Experiments* (Springer-Verlag, New York, 2003).

[37] M. Matsumoto and T. Nishimura, Mersenne twister: A 623-dimensionally equidistributed uniform pseudo-random number generator, ACM Trans. Model. Comput. Simul. **8**, 3 (1998).

[38] V. Sadovnichy, A. Tikhonravov, V. Voevodin, and V. Opanasenko, in *Contemporary High Performance Computing: From Petascale toward Exascale*, edited by J. S. Vetter (CRC Press, Boca Raton, 2013), pp. 283–307.

[39] A. V. Kargovsky, Mean density of level crossings whose duration exceeds a certain value for a low-friction nonlinear oscillator, Phys. Rev. E **86**, 061114 (2012).

[40] L. U. Ancarani and G. Gasaneo, Derivatives of any order of the confluent hypergeometric function ${}_1F_1(a,b,z)$ with respect to the parameter a or b, J. Math. Phys. **49**, 063508 (2008).